energies

MDPI

Article

How Can Floor Covering Influence Buildings' Demand Flexibility?

Hyeunguk Ahn *, Jingjing Liu, Donghun Kim, Rongxin Yin, Tianzhen Hong and Mary Ann Piette

Lawrence Berkeley National Laboratory, Building Technology and Urban Systems Division, Berkeley, CA 94720, USA; JingjingLiu@lbl.gov (J.L.); DonghunKim@lbl.gov (D.K.); RYin@lbl.gov (R.Y.); THong@lbl.gov (T.H.); MAPiette@lbl.gov (M.A.P.)

* Correspondence: hahn@lbl.gov

Abstract: Although the thermal mass of floors in buildings has been demonstrated to help shift cooling load, there is still a lack of information about how floor covering can influence the floor's load shifting capability and buildings' demand flexibility. To fill this gap, we estimated demand flexibility based on the daily peak cooling load reduction for different floor configurations and regions, using EnergyPlus simulations. As a demand response strategy, we used precooling and global temperature adjustment. The result demonstrated an adverse impact of floor covering on the building's demand flexibility. Specifically, under the same demand response strategy, the daily peak cooling load reductions were up to 20–34% for a concrete floor whereas they were only 17–29% for a carpet-covered concrete floor. This is because floor covering hinders convective coupling between the concrete floor surface and the zone air and reduces radiative heat transfer between the concrete floor surface and the surrounding environment. In hot climates such as Phoenix, floor covering almost negated the concrete floor's load shifting capability and yielded low demand flexibility as a wood floor, representing low thermal mass. Sensitivity analyses showed that floor covering's effects can be more profound with a larger carpet-covered area, a greater temperature adjustment depth, or a higher radiant heat gain. With this effect ignored for a given building, its demand flexibility would be overestimated, which could prevent grid operators from obtaining sufficient demand flexibility to maintain a grid. Our findings also imply that for more efficient grid-interactive buildings, a traditional standard for floor design could be modified with increasing renewable penetration.

Keywords: demand response; precooling; thermal inertia; cooling load; grid-interactive building

Citation: Ahn, H.; Liu, J.; Kim, D.; Yin, R.; Hong, T.; Piette, M.A. How Can Floor Covering Influence Buildings' Demand Flexibility? *Energies* **2021**, *14*, 3658. https://doi.org/10.3390/en14123658

Academic Editor: Korjenic Azra

Received: 7 May 2021
Accepted: 15 June 2021
Published: 19 June 2021

1. Introduction

Expanding the use of renewable energy, such as solar and wind energy, in an electrical grid requires higher operational flexibility to balance the supply and demand [1,2]. The demand response can enhance this operational flexibility at a low cost [3]. According to the Federal Energy Regulatory Commission, demand response is defined as "the ability of customers to respond to either a reliability trigger or a price trigger from their utility system operator, load-serving entity, regional transmission organization/independent system operator, or other demand response provider by lowering their power consumption" [4]. By participating in demand response, the commercial sector may provide significant demand flexibility—defined as the capability provided by distributed energy resources including demand response to reduce, shed, shift, and modulate electricity demand or consumption [5]—to grids because it is responsible for 36% of the total electricity consumption in the United States [6].

To improve demand flexibility, precooling and cooling setpoint temperature adjustments have been widely used. An experiment study of two office buildings in Northern California demonstrated that a combination of precooling and cooling temperature setpoint adjustment achieved more than an 80% reduction in chiller power during the peak period (2–5 PM) compared to a conventional strategy (e.g., night setback control), without compromising occupants' thermal comfort [7]. With the same demand response strategy,

another experimental study in Iowa showed that the peak cooling load during 1–5 PM decreased by 30% for a multi-purpose commercial building [8].

When using such a precooling strategy, demand flexibility can be enhanced by thermal mass in buildings. For example, Braun (1990) found that the building's thermal mass—such as walls, interior partitions, floors, ceilings, windows, and furnishings—is one of the five key factors determining the precooling effect on the peak electric load reduction and cost savings [9]. Aste et al. (2015) demonstrated that with the same precooling strategy, a cooling energy reduction for a medium-heavy mass building was 30% greater than that for a light mass building [10]. Henze et al. (2007) reported a similar pattern for operating costs [11]; however, they found that a cost saving increased only until a certain level of thermal mass and then decreased after this threshold level. They concluded that beyond this threshold level, a base cooling load (i.e., cooling load without precooling) decreased drastically, thus limiting an opportunity for a precooling strategy to further reduce cooling load and operating costs. Moreover, Turner et al. (2015) demonstrated that precooling structural thermal mass in residential buildings for various climates in the U.S. could help shift more than 50% of cooling load from an on-peak to off-peak price period [12].

As provided in Table 1, a structural floor in a building has been extensively used as thermal mass in previous demand flexibility studies. However, a structural floor is not often exposed to a zone. For example, a concrete slab can be covered by a suspended ceiling, a carpet, or furniture in a zone, which can influence the zone's cooling and heating loads and occupants' thermal comfort [13–15]. Nevertheless, none of the previous studies investigated how a covered floor can influence demand flexibility and how this influence varies with climates. Without a comprehensive understanding of this, the advantage of thermal mass on demand flexibility cannot be fully realized. Then, building operators may not be able to provide the committed demand flexibility and grid operators may suffer from balancing the electricity supply and demand during demand response events. To maintain a reliable grid, it is crucial for both building and grid operators to understand how floor covering can affect demand flexibility.

The objective of this study is to examine how floor covering influences the load shifting capability of a floor's thermal mass and buildings' demand flexibility. For a small office building, we evaluated demand flexibility for a concrete floor and a carpet-covered concrete floor. To account for climates' effects on demand flexibility, we considered two climate zones: the hot and dry and warm and marine climate. For each floor configuration and climate, we implemented precooling and global temperature adjustment as a demand response strategy. In this paper, demand response is not limited to load shedding during an electrical contingency event. Rather, it includes load shifting in response of utility tariff structures (e.g., time-of-use) such as precooling, which aligns with the definition used by a recent framework investigating interactions between demand response and energy efficiency resources [16]. Additionally, we analyzed how the behavior of floor surface temperature varies with floor configurations and how the carpet-covered area or internal heat gain influences demand flexibility.

Table 1. Previous demand flexibility studies using thermal mass.

Reference	Method	Building Type	Demand Response	Thermal Mass
Braun (1990) [9]	Simulation	Single-zone building	Precooling	Floor, exterior and partition walls, and ceiling
Rabl and Norford (1991) [17]	Simulation	Multi-story office building	Night ventilation	Floor, walls, and ceiling
Kintner-Meyer and Emery (1995) [18]	Simulation	Multi-story office building	Precooling	Floor, exterior walls, and ceiling
Becker and Paciuk (2002) [19]	Simulation	Multi-story office building	Precooling and night ventilation	Floor, exterior, interior, and partition walls
Zhou et al. (2005) [20]	Simulation	Multi-story office building	Precooling and night ventilation	Floor, exterior walls, roof, and ceiling
Xu and Haves (2006) [7]	Measurement and simulation	Multi-story office building	Precooling and cooling setpoint temperature adjustment	Floor and exterior walls

Table 1. *Cont.*

Reference	Method	Building Type	Demand Response	Thermal Mass
Henze et al. (2007) [11]	Simulation	Multi-story office building	Precooling	Floor, exterior and interior walls, roof, and ceiling
Lee and Braun (2008) [8]	Measurement and simulation	Multi-purpose commercial building (office and classroom)	Precooling and cooling setpoint temperature adjustment	Floor, exterior and interior walls, and roof
Yang and Li (2008) [21]	Simulation	Single-zone building	Night ventilation	Exterior walls
Aste et al. (2015) [10]	Simulation	Multi-story office building	Night ventilation and adaptive shading	Floor, walls, and roof
Chen et al. (2019) [22]	Simulation	Multi-story office building	Cooling setpoint temperature adjustment, light dimming, and electric appliances' operation shifting	Floor, exterior and partition walls, ceiling, and furniture
Panão et al. (2019) [23]	Simulation	Apartment building and passive house	Preheating	Floor and ceiling

2. Methodology

To perform parametric analyses for thermal and physical properties of different materials in floor layers, we used jEPlus which is an open-source research tool that implements complex parametric runs with EnergyPlus models [24]. EnergyPlus is described in Section 2.1. We used the U.S. Department of Energy (DOE)'s reference small office building model, as described in Section 2.2. Sections 2.3–2.6 describe the simulated cases, examined floor configurations, examined demand response strategy, and evaluation criteria for demand flexibility.

2.1. Description of EnergyPlus

EnergyPlus is the U.S. DOE's building energy simulation software [25]. An EnergyPlus simulation calculates a building's cooling and heating loads, energy consumption, occupant comfort, and energy costs. EnergyPlus has been widely used to support development of building energy codes and standards, code compliance, performance rating, and the design and operation of energy efficient buildings. Because EnergyPlus assumes one-dimensional heat transfer, the surface temperature is uniform. EnergyPlus has been verified according to ASHRAE Standard 140, Standard Method of Test for Building Energy Simulation Computer Programs. Additionally, EnergyPlus has shown a reasonable agreement with experiments in existing literature [26–29].

2.2. Description of the DOE's Reference Small Office Building Model

According to the 2012 Commercial Buildings Energy Consumption Survey, office buildings consume about 16% of the total electricity in the U.S. commercial sector and more than 50% of them are small-sized (i.e., a floor area less than 460 m^2 or 5000 ft^2) [30]. For this reason, we used the DOE's reference small office building for a simulation study, which also allows comparing our results with other studies. Table 2 describes the DOE's reference small office building model.

Table 2. Description of the DOE's reference small office building model. Reproduced from [31], National Renewable Energy Laboratory: 2011.

Building Characteristic	Description
Building type	Small Office
Vintage	ASHRAE Standard 90.1-2004
Location	Phoenix, AZ (climate zone 2B); San Francisco, CA (climate zone 3C)
Floor area	510 m^2
No. of floors	1
Zones	1 core zone and 4 perimeter zones
Aspect ratio	1.5
Window fraction	24.4% for South perimeter zone and 19.8% for North, East, and West perimeter zones
Cooling system	Air-source heat pump
Air distribution	Single-zone constant air volume (CAV)

The simulated buildings were located in the hot and dry climate of Phoenix, AZ and the warm and marine climate of San Francisco, CA [32]. Due to the low humidity levels in these climates, a sensible cooling load contributes largely to the buildings' cooling loads and it is a strong function of outdoor dry-bulb temperature and internal heat gains. We performed hourly energy simulations for the summer period (June to October). Using Typical Meteorological Year (TMY) data for these locations, we calculated hourly average dry-bulb temperature during that period. For more than 1000 locations in the U.S., TMY data are derived from 1991–2005 historical data to represent the normal hourly values of solar radiation and meteorological elements for a one-year period [33]. Figure 1 shows that the hourly average dry-bulb temperature for Phoenix is about 10 to 20 °C higher than that for San Francisco during the examined period.

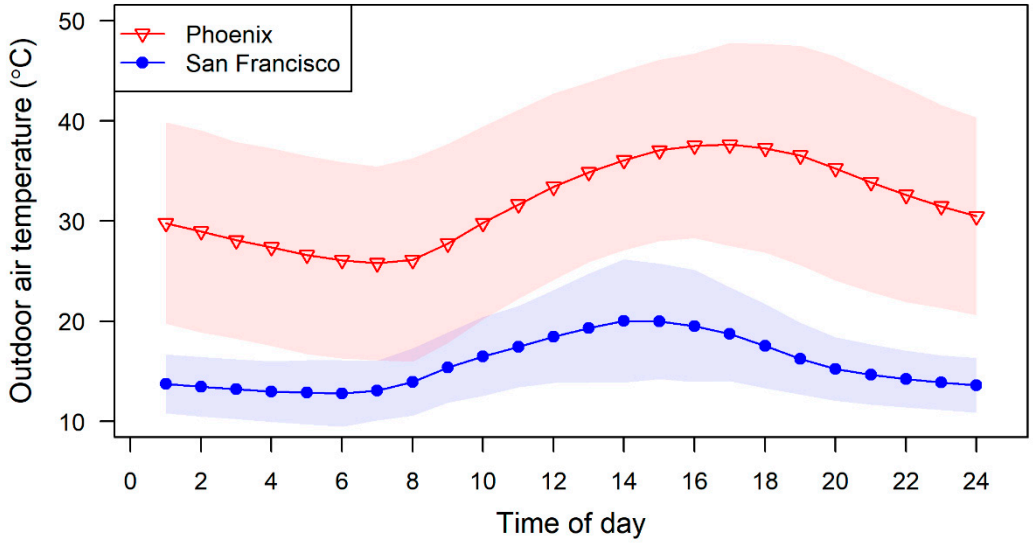

Figure 1. Hourly average outdoor dry-bulb temperature in Phoenix, AZ and San Francisco, CA during 106 weekdays from 1 June to 31 October. Shaded areas indicate above and below two standard deviations from the estimated mean.

Regardless of the location, the internal heat gains from occupants, lights, and electric equipment were kept the same. EnergyPlus estimates heat gains from occupants using floor area per person (i.e., m^2/person) and those from lights and electric equipment using heat intensity (i.e., W/m^2); thus, the total internal heat gains were determined by the floor area. However, convective and radiant heat fractions varied depending on the type of internal heat gains. For example, both convective and radiant heat fractions were 0.5 for occupants and electric equipment, whereas the fractions for lights were 10% convection, 70% long-wave radiation, and 20% short-wave (visible) radiation. These inputs are summarized in Table 3. The hourly schedules of occupancy, lighting, and electric equipment are shown in Figure 2.

Table 3. Detailed inputs for internal heat gains. Reproduced from [31], National Renewable Energy Laboratory: 2011.

Internal Heat Gains	Intensity (W/m^2)	Convective Fraction	Radiant Fraction	Visible Fraction
Occupants	6.46 (1)	0.5	0.5	0
Lights	10.76	0.1	0.7	0.2
Electric equipment	10.76	0.5	0.5	0

(1) Heat intensity for occupants was calculated by dividing 120 W/person (sensible and latent load for each person) by 18.58 m^2/person (floor area per person).

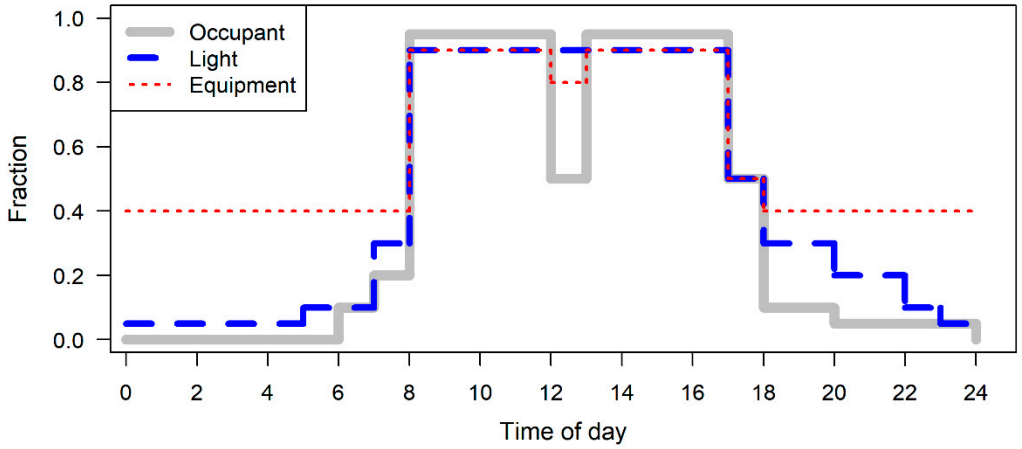

Figure 2. Hourly fraction schedules of internal heat gains including occupants, lights, and electric equipment during weekdays. The fraction of 1.0 indicates the full intensity for each internal heat gain which is provided in Table 3.

2.3. Description of Simulated Cases

We simulated a total of 12 cases as combinations of three floor configurations using two cooling strategies for two climate zones. These simulated cases are summarized in Table 4. Note that the first letters of floor configurations and cooling strategies are capitalized for the remainder of this paper to indicate the case name. Details of the examined floor configurations and cooling strategies are described in the following sections.

Table 4. Summary of simulated cases.

Case No.	Climate Zone	Cooling Strategy	Floor Configuration	Simulation Duration
1	Phoenix, AZ (hot and dry)	Base	Bare concrete	1 June–31 Oct
2			Concrete + carpet	
3			Wood	
4		Precooling + GTA	Bare concrete	
5			Concrete + carpet	
6			Wood	
7	San Francisco, CA (warm and marine)	Base	Bare concrete	
8			Concrete + carpet	
9			Wood	
10		Precooling + GTA	Bare concrete	
11			Concrete + carpet	
12			Wood	

2.4. Description of Floor Configurations

To investigate the effects of floor covering on demand flexibility, we mainly compared an exposed concrete floor (Bare concrete) and a carpet-covered concrete floor (Concrete + carpet). As a reference for low thermal mass, we also considered a wood floor (Wood). Figure 3 illustrates the cross-sectional views of the three floor configurations. Because the effects of thermal mass can greatly depend on heat transfer with external environment [19], we added a 5 cm slab insulation at the bottom of all the floor configurations to minimize heat transfer with the ground while focusing on the heat transfer between the zone and floor. All other inputs in the DOE's reference model—exterior and interior walls, windows, ceilings, roof, coefficient of performance of the air-source heat pump, infiltration rate, and minimum outdoor air ventilation rate—stayed unchanged.

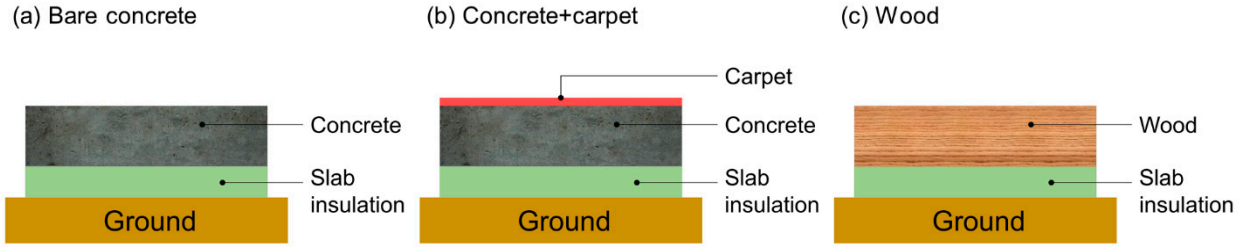

Figure 3. Cross-sectional views of the three examined floor configurations: (**a**) Bare concrete, (**b**) Concrete + carpet, and (**c**) Wood.

These floor configurations were modeled using thermal and physical properties including thermal conductivity, density, specific heat, and thickness [31,34]. Detailed inputs for these properties are summarized in Table 5. For all floor configurations, the surface thermal absorptivity was 0.9. Such thermal properties of floor materials can determine the delay effect when converting radiant heat gains absorbed to the floor surface to convective heat (i.e., cooling load). EnergyPlus manages this delay effect using a decay curve [35].

Table 5. Thermal and physical properties of materials in floor layers.

Floor Layer	Conductivity (W/mK)	Density (kg/m^3)	Specific Heat (J/kgK)	Thickness (cm)
Concrete	1.311	2240	836.8	10
Wood	0.12	540	1210	10
Slab insulation	0.035	265	1300	5
Carpet (synthetic)	0.060	160	2500	1

2.5. Description of Cooling Strategies

As a demand response measure, we implemented a Precooling + GTA strategy. A GTA strategy raises the cooling temperature setpoint globally across all the zones in a building during a demand response event [36]. Figure 4 illustrates the cooling setpoint schedules used in two cooling strategies: Base and Precooling + GTA. Compared to the Base scenario, the temperature setpoint decreased by 1 °C during the precooling period (i.e., 6 AM–noon) and increased by 1 °C during the GTA period (i.e., noon–6 PM). The GTA period reflects the typical peak price time window in a time-of-use rate in the U.S. [37].

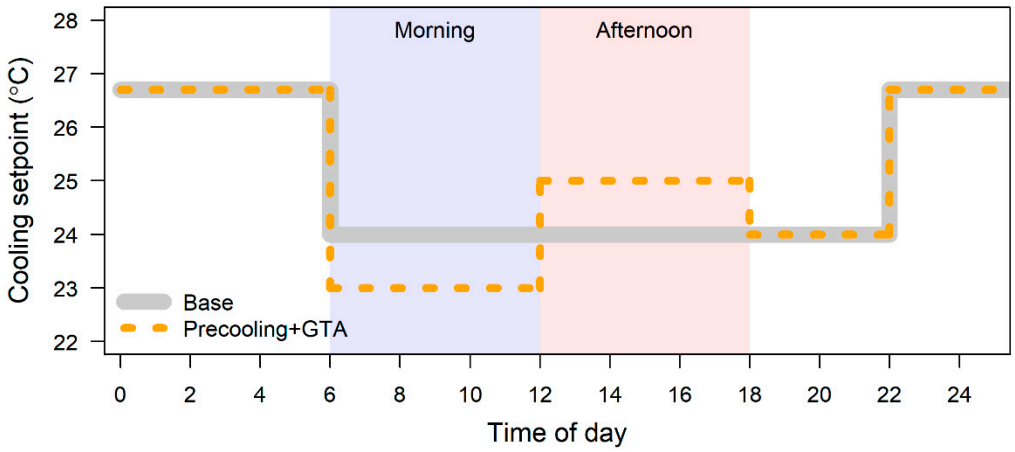

Figure 4. Cooling temperature setpoint schedules for Base and Precooling + GTA scenarios.

2.6. Evalation Criteria for Demand Flexibility

To evaluate the building's demand flexibility, we compared hourly cooling loads and the daily peak cooling load for the Precooling + GTA scenario compared to those for the Base scenario. We focused on cooling load reductions during the GTA period (i.e.,

noon–6 PM). A similar approach was used by many previous studies [8,10,19]. To eliminate disturbance on results due to different weekend schedules, we focused only on weekdays from 1 June to 31 October. A variation in an hourly cooling load at *i*-th hour ($\Delta cooling_i$) can be expressed as

$$\Delta cooling_i = cooling_{i,Precooling+GTA} - cooling_{i,Base} \quad (1)$$

where *i* indicates hour of the day and $cooling_{i,Precooling+GTA}$ and $cooling_{i,Base}$ indicate cooling loads (kW) at the *i*-th hour for the Precooling + GTA and Base scenarios, respectively.

Similarly, a variation in the daily peak cooling load on the *n*-th day ($\Delta peak\ cooling_n$) was estimated as

$$\Delta peak\ cooling_n = peak\ cooling_{n,Precooling+GTA} - peak\ cooling_{n,Base} \quad (2)$$

where $peak\ cooling_{n,Precooling+GTA}$ and $peak\ cooling_{n,Base}$ indicate the daily peak cooling loads (kW) on the *n*-th weekday for the Precooling + GTA and Base scenarios, respectively. Because the daily peak cooling load mostly occurred at 4 PM for the examined building, its reduction can help determine potential savings on operating costs, especially when there is a significant demand charge component in electricity rates [9,38].

3. Sensitivity Analysis

3.1. Sensitivity of Carpet-Covered Area to Demand Flexibility

Even for the same Precooling + GTA strategy, demand flexibility may vary depending on the floor covering area. Thus, we varied a ratio of the carpet-covered area to the total floor area from 20% to 80% by a 20-unit increase in percent in each zone. This sensitivity analysis was only performed for the concrete floor configuration.

3.2. Sensitivity of Temperature Adjustment Depth to Demand Flexibility

Because the daily peak cooling load reduction can be greatly influenced by the depth of the cooling setpoint temperature adjustment during the GTA period, we considered three levels of cooling setpoint temperature adjustments: 0 °C, 1 °C, and 2 °C. Note that in the original simulation cooling setpoint temperature was adjusted moderately by 1 °C. Thus, the temperature adjustment by 0 °C represents no GTA or a less intensive GTA case and the temperature adjustment by 2 °C represents a more intensive GTA case.

4. Results and Discussion

4.1. Hourly Cooling Load Profiles

Comparisons of hourly cooling load profiles for different floor configurations and cooling scenarios are provided in Figure 5 (Phoenix, AZ, USA) and Figure 6 (San Francisco, CA, USA). Figures 5c and 6c determine demand flexibility using the change of hourly cooling loads for the Precooling + GTA scenario compared to the Base scenario. Because a negative value indicates a reduction in the hourly cooling load compared to the Base scenario, the lower value represents the higher demand flexibility during the GTA period (i.e., noon–6 PM). For all floor configurations hourly cooling loads sharply drop at noon when cooling setpoint temperature increases by 1 °C; thus, cooling load reductions during 1–6 PM are mainly discussed.

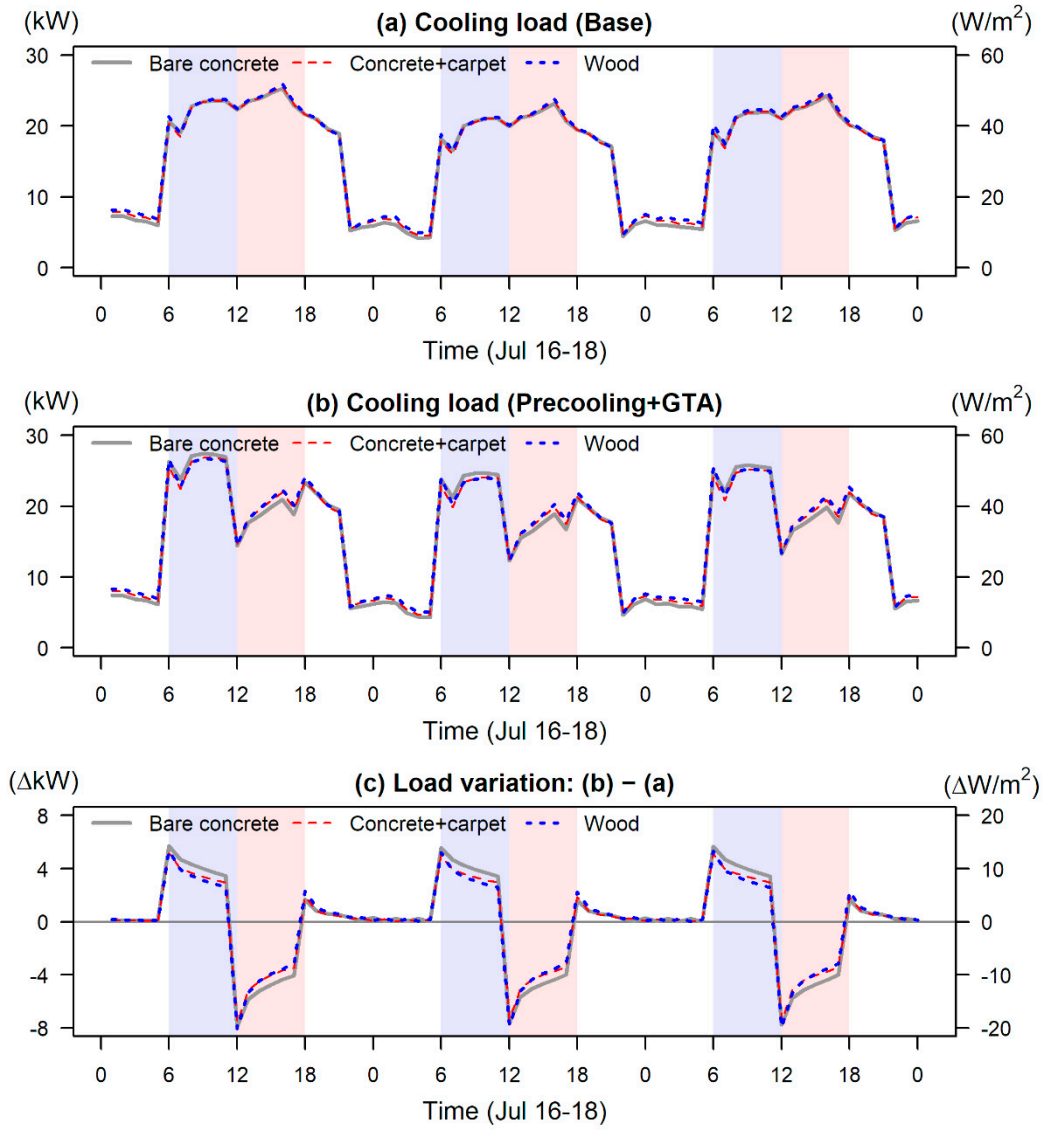

Figure 5. Hourly cooling loads for three floor configurations: Bare concrete, Concrete + carpet, and Wood under (**a**) Base and (**b**) Precooling + GTA scenarios, and (**c**) variations in hourly cooling loads between the two scenarios during 16–18 July in Phoenix, AZ. The blue-shaded area indicates the morning or precooling period while the red-shaded area indicates the afternoon or GTA period.

For both Phoenix and San Francisco, adding a carpet notably reduces the building's demand flexibility during 1–6 PM. Note that for San Francisco Bare concrete reduces cooling load by a comparable amount (3–4 kW) with Concrete + carpet despite a lower base cooling load, indicating a higher demand flexibility. For Phoenix where a small diurnal variation in outdoor temperature could limit the effective use of thermal mass on load shifting [21,39], a cooling load reduction is consistently lower by 1 kW for Concrete + carpet than that for Bare concrete. Additionally, the pattern for Concrete + carpet is almost same as that for Wood, indicating that floor covering could negate load shifting capability of a concrete floor, especially in hot climates.

Due to precooling, cooling load increases during 6 AM–noon, which may increase daily net energy consumption [19]. However, our supplemental analysis shows that the daily net energy consumption marginally varies between the Base and Precooling + GTA scenarios for all floor configurations (see Figures S1 and S2 in Supplementary Materials).

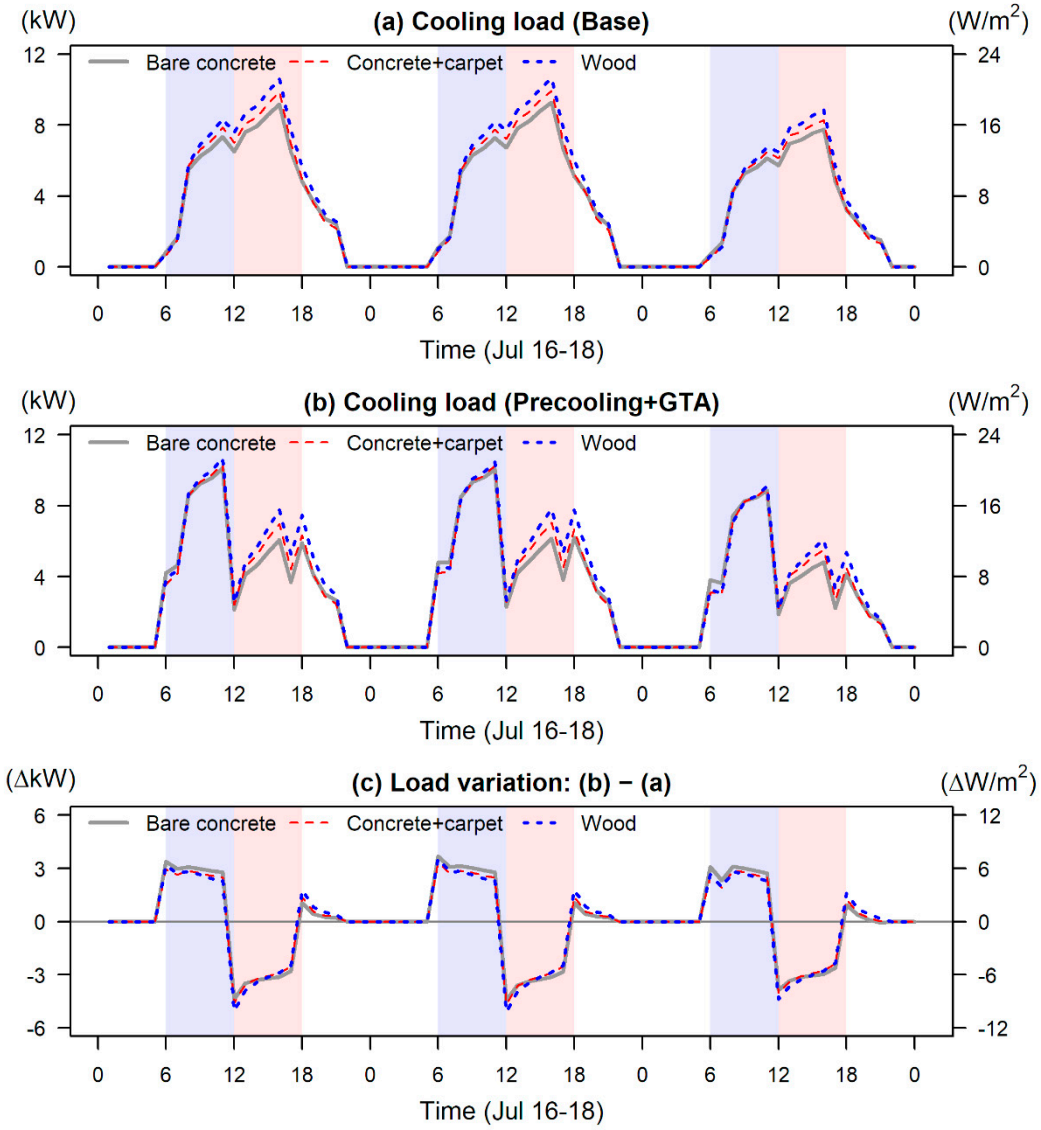

Figure 6. Hourly cooling loads for three floor configurations: Bare concrete, Concrete + carpet, and Wood under (**a**) Base and (**b**) Precooling + GTA scenarios, and (**c**) variations in hourly cooling loads between the two scenarios during 16–18 July in San Francisco, CA. The blue-shaded area indicates the morning or precooling period while the red-shaded area indicates the afternoon or GTA period.

4.2. Floor Surface Temperature

To elucidate the cooling load behaviors, we investigated floor surface temperatures for the three floor configurations. To exclude the influence of solar radiation on the floor surface temperature, we only used the core zone. Figures 7 and 8 present the results of Phoenix and San Francisco cases, respectively. The floor surface temperatures for San Francisco are consistently lower by 1.5–3 °C than those for Phoenix due to the minimum ventilation air requirement that induces cool outdoor air into the zone while providing free cooling.

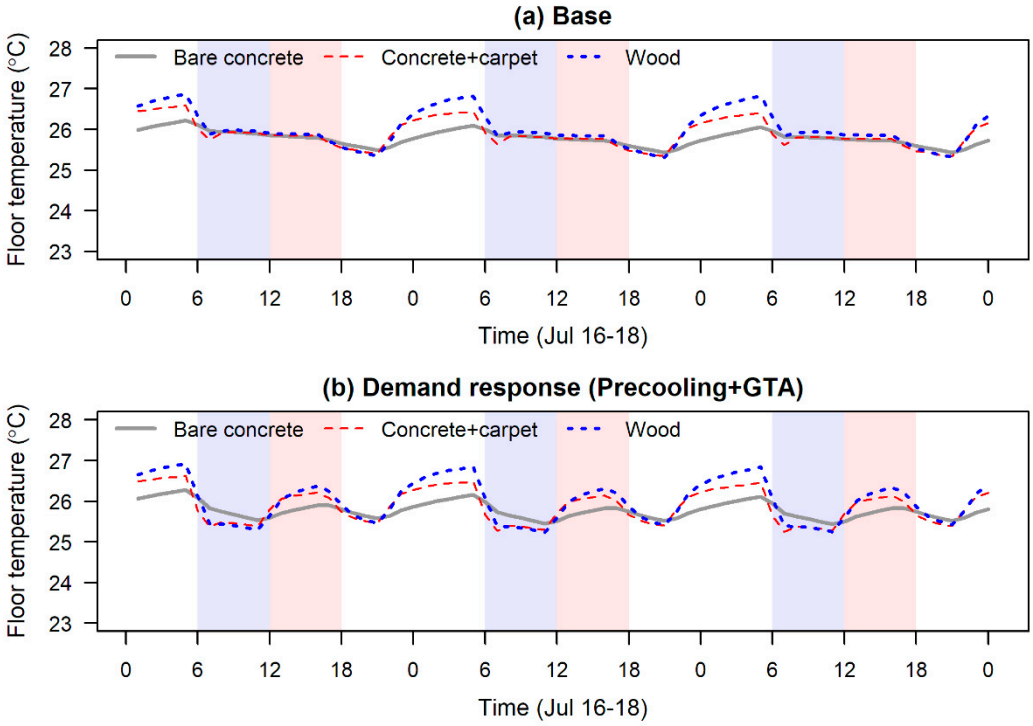

Figure 7. Hourly floor surface temperature of the core zone for three floor configurations: Bare concrete, Concrete + carpet, and Wood under (**a**) Base and (**b**) Precooling + GTA scenarios during 16–18 July in Phoenix, AZ. The blue-shaded area indicates the morning or precooling period while the red-shaded area indicates the afternoon or GTA period.

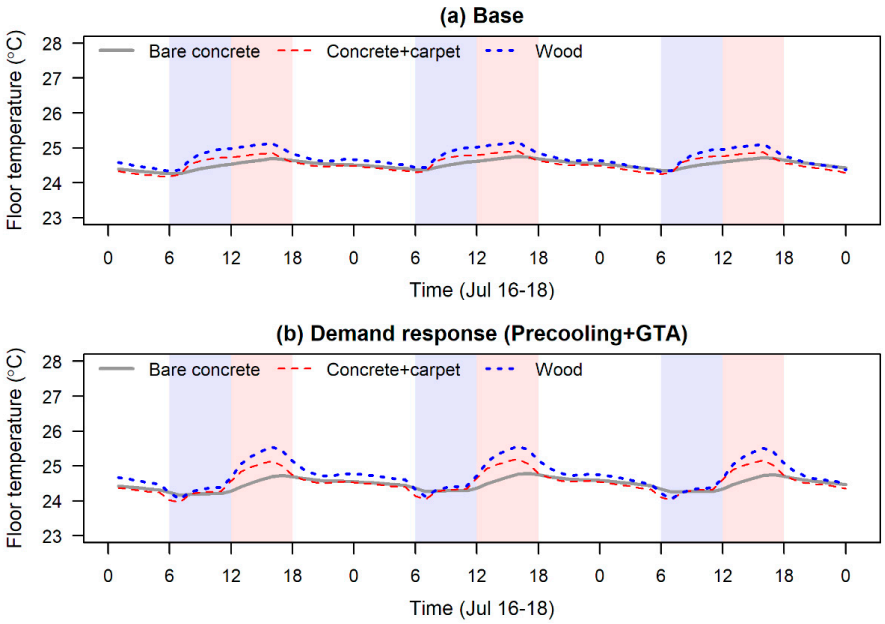

Figure 8. Hourly floor surface temperature of the core zone for three floor configurations: Bare concrete, Concrete + carpet, and Wood under (**a**) Base and (**b**) Precooling + GTA scenarios during 16–18 July in San Francisco, CA. The blue-shaded area indicates the morning or precooling period while the red-shaded area indicates the afternoon or GTA period.

For Bare concrete, the zone air is strongly coupled with the concrete floor. However, this convective coupling is weakened by adding a carpet. As a result, the floor surface temperature for Concrete + carpet varies within a wider range (<2 °C) than that for Bare concrete (<1 °C). The consistent floor surface temperature for Bare concrete is due to concrete's low thermal diffusivity [40] and leads to a high thermal time constant [14,41].

These physical attributes help keep the floor surface temperature constantly lower than the zone air temperature during the GTA period (i.e., noon–6 PM), resulting in a higher demand flexibility than Concrete + carpet (see Figures 5c and 6c). Additionally, the lower floor surface temperature for Bare concrete enables absorbing the greater amount of long-wave radiation, contributing to a higher demand flexibility (see Figures S3 and S4 in Supplementary Materials).

Because floor surface temperature determines zone operative temperature [7], floor covering may also influence occupants' thermal comfort (see Figures S5 and S6 in Supplementary Materials). Compared to Bare Concrete, Concrete + carpet tends to achieve a lower floor surface temperature during the precooling period and a higher floor surface temperature during the GTA period, which may reduce occupants' thermal comfort. Therefore, to provide a comparable thermal comfort level with Bare concrete, Concrete + carpet may require less cooling energy during the precooling period and more cooling energy during the GTA period. Future research may investigate how this cooling energy tradeoff could influence the daily net energy consumption for Concrete + carpet.

4.3. Daily Peak Cooling Load

The investigation of the daily peak cooling load reduction aids the grid operators to estimate buildings' demand flexibility and the building owners to estimate potential cost savings. Figure 9 shows absolute and relative reductions of the daily peak cooling loads for the three floor configurations in San Francisco and Phoenix.

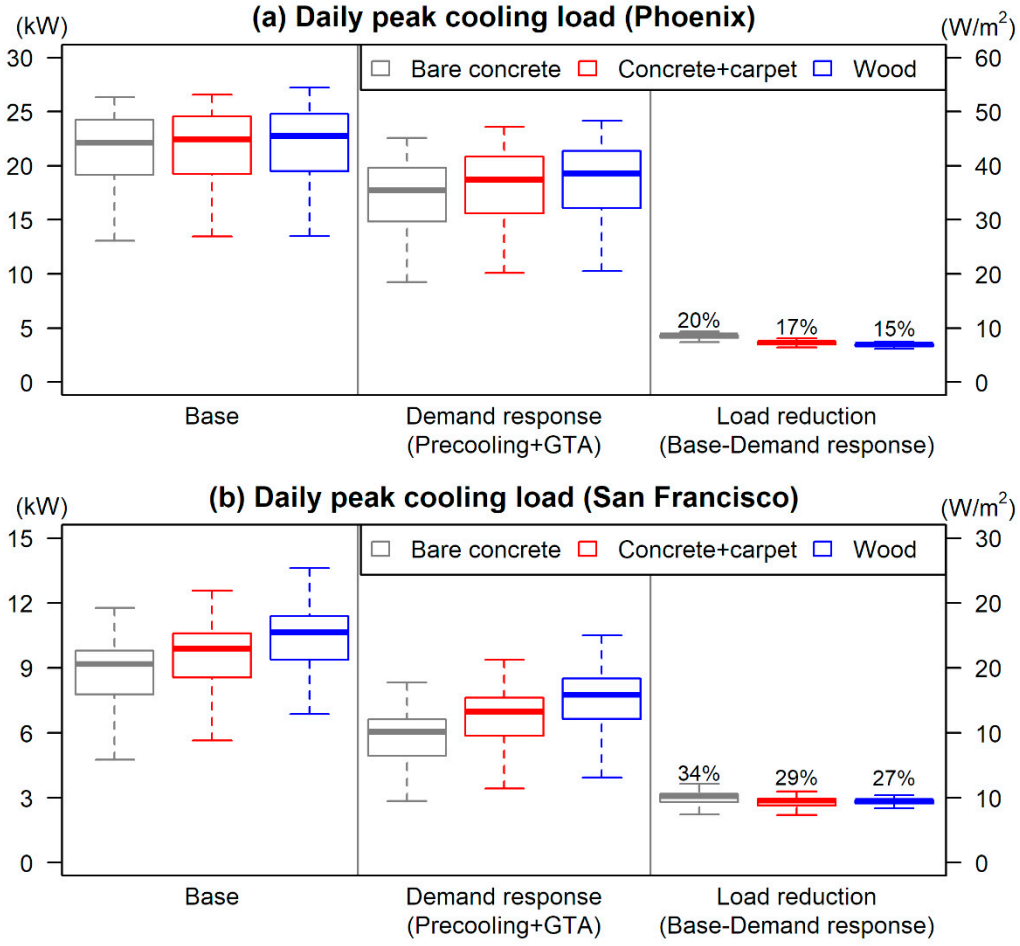

Figure 9. The daily peak cooling loads for the Base and Precooling + GTA scenarios and the reductions compared to the Base scenario for three floor configurations: Bare concrete, Concrete + carpet, and Wood during 106 weekdays from 1 June to 31 October in (**a**) Phoenix, AZ and (**b**) San Francisco, CA. The percentage above a box indicates the median of relative reductions compared to the Base scenario.

Relative daily peak cooling load reductions for Bare concrete range from 20% to 34% whereas those for Concrete + carpet range from 17% to 29%. Although these ranges are not significantly different, a difference in electricity cost savings for the two floor configurations would be greater because time-of-use rates in the U.S. often have a 2–3 times higher demand charge (USD/kW) during a peak period than an off-peak period [37]. For example, with a PG&E time-of-use rate for San Francisco, a saving in a monthly demand charge is about 10% greater for Bare concrete (55 USD saving per month) compared to Concrete + carpet (51 USD saving per month). Additionally, the result indicates that the benefit of high thermal mass (e.g., concrete) on improving demand flexibility—demonstrated by several previous studies [10,11]—can be realized only when the thermal mass is exposed to a zone. If this factor is not considered in estimating demand flexibility especially for heavy-concrete buildings, the result could be overestimated as concrete is not often exposed to a zone in real buildings. This overestimation could further increase for aggregated buildings, which could lead to a significant hurdle for grid operators to predict potential demand flexibility from buildings.

Regarding the climate, an absolute reduction is greater for Phoenix (~5 kW) than that for San Francisco (~3 kW). However, due to a lower base cooling load for San Francisco a relative reduction is greater (27–34%) than that for Phoenix (15–20%). From the building's point of view, a greater relative reduction in moderate climates (e.g., San Francisco) can lead to a greater cost saving when implementing a demand response strategy. However, grid operators can expect higher demand flexibility from buildings in hotter climates (e.g., Phoenix). This result agrees well with a previous study showing that demand flexibility of commercial buildings increased with higher outdoor temperature [42].

4.4. Sensitivity of Floor Covering Area to Demand Flexibility

To examine the sensitivity of a floor covering area to demand flexibility, for both the Base and Precooling + GTA scenarios we varied the ratio of carpet-covered area to the total floor area from 20% to 80% for all zones in the building. Figure 10 shows the daily peak cooling load reduction compared to each Base scenario for each carpet-covered area ratio. The percentage above each box indicates a relative reduction compared to each Base scenario.

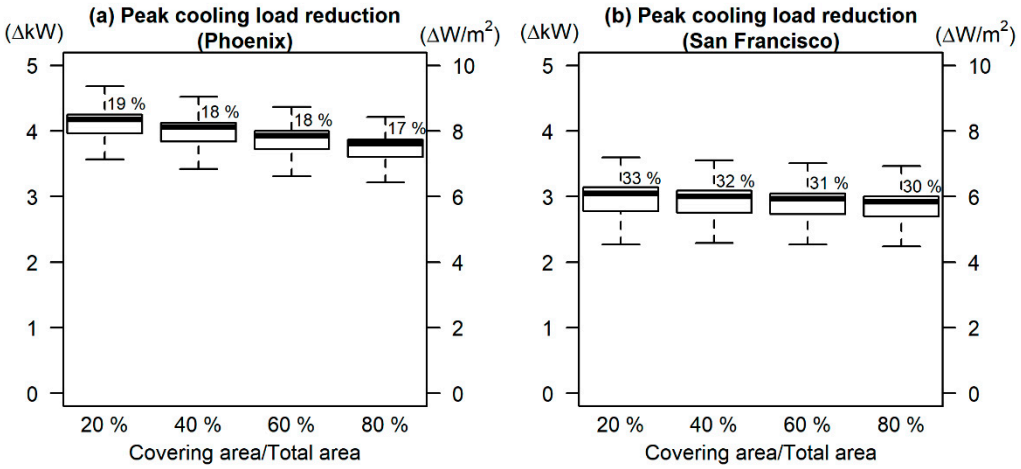

Figure 10. Sensitivity of the carpet-covered area to the peak cooling load reduction for a concrete floor in (**a**) Phoenix, AZ and (**b**) San Francisco, CA. The ratio of the carpet-covered area to the total area was varied from 20% to 80% uniformly across all zones in the building. The peak cooling load reductions were estimated during 106 weekdays from 1 June to 31 October. The percentage above a box indicates the median of relative reductions compared to the Base scenario.

For both climates, a peak cooling load reduction decreases with a larger carpet-covered area, indicating a lower demand flexibility. While both absolute and relative reductions noticeably decrease as the carpet-covered area increases in Phoenix, an absolute reduction

decreases only by less than 0.1 kW in San Francisco. This is mainly due to a lower base cooling load in San Francisco (see Figure 9b). A pattern of relative peak cooling load reductions—decreasing from 33% to 30% with increasing carpet-covered area—clearly shows a notable effect of floor covering on demand flexibility. This result implies that if a floor's thermal mass is covered by furniture or partition walls, which is very common in real buildings, demand flexibility can decrease compared to a case with an exposed floor. Note that furniture or partition walls could contribute to increasing demand flexibility if they are composed of a high thermal mass material [22].

4.5. Sensitivity of GTA Depth to Demand Flexibility

Figure 11 shows a strong linear relationship between the GTA depth and daily peak cooling load reduction regardless of the floor configuration. The figure also demonstrates that the negative impact of floor covering on demand flexibility can be more profound with a greater depth of GTA. Specifically, at the GTA depth of 1 °C the differences in the daily peak cooling load reductions between Bare concrete and Concrete + carpet are Δ0.32 kW for Phoenix and Δ0.20 kW for San Francisco, whereas at the GTA depth of 2 °C those are Δ0.42 kW for Phoenix and Δ0.26 kW for San Francisco.

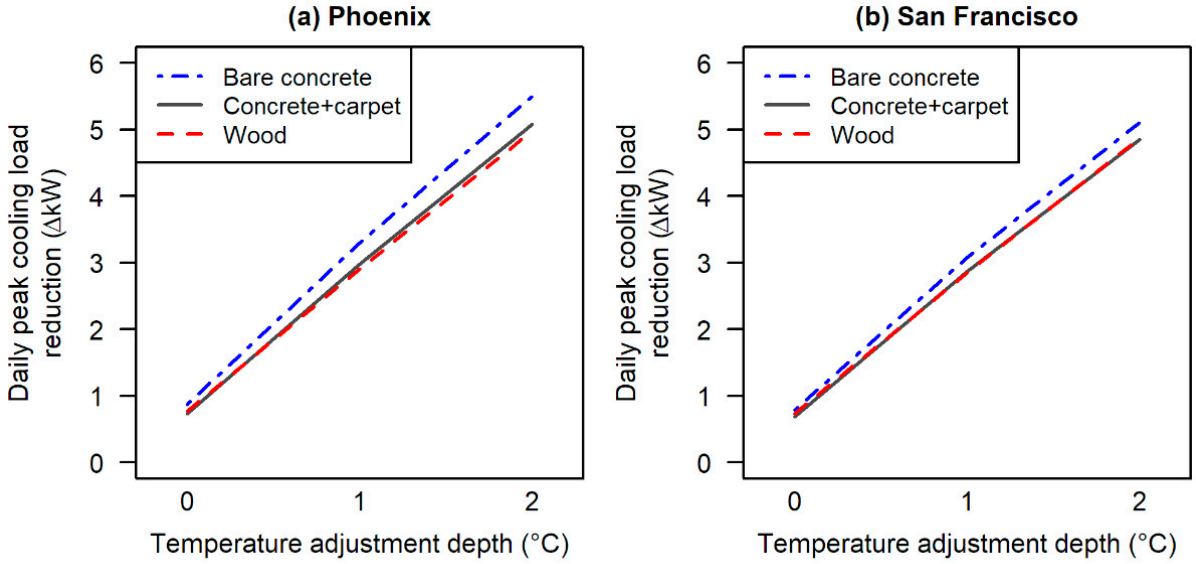

Figure 11. A median value of the daily peak cooling load reductions during 106 weekdays from 1 June to 31 October with respect to the GTA depth for three floor configurations: Bare concrete, Concrete + carpet, and Wood in (**a**) Phoenix, AZ and (**b**) San Francisco, CA.

5. Further Discussion about Convective and Radiant Fractions of Internal Heat Gains

Our analysis shows that floor covering can significantly reduce demand flexibility of a building. A previous study demonstrated that demand flexibility depends largely on the amounts of internal heat gains [19]. However, because sensible heat gains are composed of convective and radiant heat gains, it is of interest to investigate which of them affects more on demand flexibility. For this reason, we varied a radiant fraction of equipment heat gains from 0.2 to 0.8. While varying a radiant fraction, the sum of convective and radiant fractions stayed constant as 1; thus, the maximum heat intensity of equipment heat gains was kept same as 10.76 W/m^2. Similar to the previous sections, we estimated absolute and relative reductions of the daily peak cooling load for the Precooling + GTA scenario compared to the Base scenario.

According to Figure 12, both absolute and relative peak cooling load reductions increase as a radiant fraction of equipment heat gains increases. Additionally, the reductions are greatest for Bare concrete. While the previous study [19] demonstrated that demand flexibility is proportional to the total amount of internal heat gains, our result finds that the

radiant component of internal heat gains can be more influential in determining demand flexibility than the convective component. This is because a radiant heat gain is absorbed to the surfaces of a floor, a ceiling, and walls, and then contributes to cooling load through the complex dynamics of building thermal network, resulting in a time delay as opposed to a convective heat gain. This result implies that thermal mass can achieve higher demand flexibility for buildings with greater radiant heat gains. Examples of such buildings could be office and retail buildings that have intensive lighting loads [43].

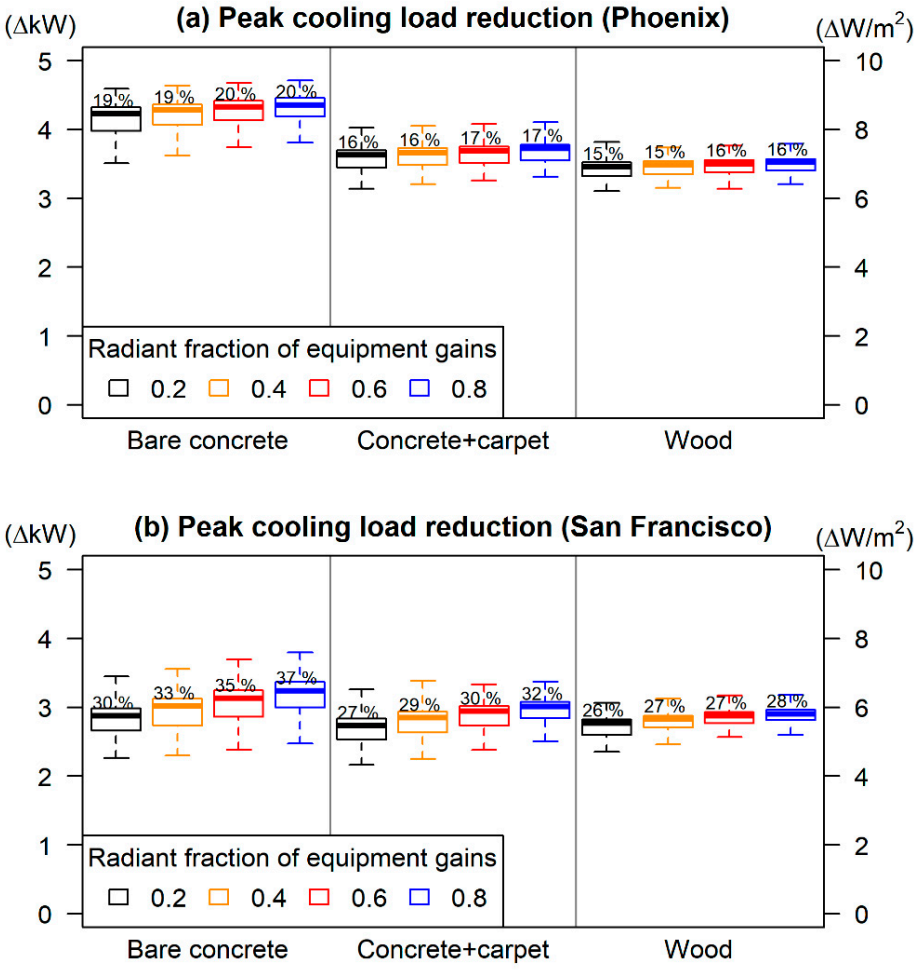

Figure 12. Sensitivity of a radiant fraction of equipment gains to the peak cooling load reduction for three floor configurations: Bare concrete, Concrete + carpet, and Wood in (**a**) Phoenix, AZ and (**b**) San Francisco, CA. The sum of the convective and radiant fractions stayed constant as one. The peak cooling load reductions were estimated during 106 weekdays from 1 June to 31 October. The percentage above a box indicates the median of relative reductions compared to the Base scenario.

6. Limitations and Future Research

Because we used the default room air model in EnergyPlus that assumes air in a zone is well mixed and has a uniform temperature, future research may use different air models in EnergyPlus or computational fluid dynamics models [44] to capture the effects of ventilation strategies (e.g., mixing and displacement) [45] on demand flexibility and occupants' thermal comfort. Additionally, future research can leverage thermal mass's demand shifting capability using advanced control strategies including model-predictive, occupant-based, and smart-zoning control [46,47]. To verify EnergyPlus in determining buildings' demand flexibility, we are performing experiments in a laboratory, which will be discussed in future research. This study focused on a single-story building and used building performance simulation to quantify how floor covering influenced demand flexibility.

For multi-story buildings, however, floor covering may help reduce cooling load and these counteracting factors may be investigated by future research. Future research may estimate a fraction of floor covering's effects on the total cooling load to those of other building envelopes including walls, windows, and roofs. Different materials of floor coverings such as ceramic, rubber, and wool may be considered by future research.

7. Conclusions

This study investigated the effects of floor covering on demand flexibility for a small office building based on reductions in the daily peak cooling load. We considered different floor configurations and climates. We found that floor covering can be a critical parameter in determining demand flexibility as it significantly prevented a floor's thermal mass from shifting cooling load from peak to off-peak periods. Under the same demand response strategy (i.e., Precooling + GTA), the daily peak cooling load reductions were only 17–29% for a carpet-covered concrete floor whereas they were up to 20–34% for a concrete floor. Compared to the reduction for a wood floor representing low thermal mass, that for a carpet-covered concrete floor was within a marginal difference (<5%). This result implies that with time-of-use rates, the effect of floor covering on electricity cost savings could be amplified. Specifically, with a time-of-use rate in San Francisco, a cost saving in a monthly demand charge could be approximately 10% greater for a concrete floor (55 USD saving per month) than for a carpet-covered concrete floor (51 USD saving per month). We also found that the building's demand flexibility increased with a smaller carpet-covered area or a higher radiant heat gain. With these findings considered, researchers can perform a series of similar investigations for various building types and climates. This could help grid operators accurately estimate buildings' demand flexibility and balance the electricity demand and supply during demand response events, maintaining reliable grids with increasing renewable penetration.

Supplementary Materials: The following are available online at https://www.mdpi.com/article/10.3390/en14123658/s1, Figure S1: Daily net cooling energy consumptions for three floor configurations: Bare concrete, Concrete + carpet, Wood under Base and Precooling + GTA scenarios in Phoenix, AZ., Figure S2: Daily net cooling energy consumptions for three floor configurations: Bare concrete, Concrete + carpet, Wood under Base and Precooling + GTA scenarios in San Francisco, CA., Figure S3: Hourly radiation heat transfer on the floor surface in the core zone for three floor configurations: Bare concrete, Concrete + carpet, and Wood under (a) Base and (b) Precooling + GTA scenarios in Phoenix, AZ. A positive indicates radiant heat is absorbed into the surface., Figure S4: Hourly radiation heat transfer on the floor surface in the core zone for three floor configurations: Bare concrete, Concrete + carpet, and Wood under (a) Base and (b) Precooling + GTA scenarios in San Francisco, CA. A positive indicates radiant heat is absorbed into the surface., Figure S5: Hourly operative temperatures of the core zone for three floor configurations: Bare concrete, Concrete + carpet, and Wood under (a) Base and (b) Precooling + GTA scenarios in Phoenix, AZ., Figure S6: Hourly operative temperatures of the core zone for three floor configurations: Bare concrete, Concrete + carpet, and Wood under (a) Base and (b) Precooling + GTA scenarios during in San Francisco, CA.

Author Contributions: Conceptualization, H.A. and J.L.; Data Curation, H.A.; Funding Acquisition, M.A.P.; Investigation, H.A. and D.K.; Methodology, H.A.; Project Administration, J.L. and M.A.P.; Software, H.A. and R.Y.; Supervision, T.H. and M.A.P.; Validation, H.A., D.K. and T.H.; Visualization, H.A.; Writing—Original Draft, H.A.; Writing—Review and Editing, H.A., J.L., D.K. and T.H. All authors have read and agreed to the published version of the manuscript.

Funding: This research was supported by the Rosenfeld Building Scientific Workforce Development Program and the Grid Interactive Efficient Buildings research under the Building Technologies Office of the Office of Energy Efficiency and Renewable Energy of the U.S. Department of Energy (DOE) under Contract No. DE-AC02-05CH11231.

Institutional Review Board Statement: Not applicable.

Informed Consent Statement: Not applicable.

Acknowledgments: The authors especially thank Amir Roth and Monica Neukomm from the DOE Building Technologies Office and Marco Pritoni from Lawrence Berkeley National Laboratory for their feedback.

Conflicts of Interest: The authors declare no conflict of interest.

References

1. Denholm, P.; Hand, M. Grid flexibility and storage required to achieve very high penetration of variable renewable electricity. *Energy Policy* **2011**, *39*, 1817–1830. [CrossRef]
2. Sun, Y.; Wachche, S.; Mills, A.; Ma, O. *2018 Renewable Energy Grid Integration Data Book*; National Renewable Energy Laboratory: Golden, CO, USA, 2020; p. 124.
3. Wang, Q.; Hodge, B.-M. Enhancing Power System Operational Flexibility with Flexible Ramping Products: A Review. *IEEE Trans. Ind. Inform.* **2017**, *13*, 1652–1664. [CrossRef]
4. Kathan, D.; Daly, C.; Eversole, E.; Farinella, M.; Gadani, J.; Irwin, R.; Lankford, C.; Pan, A.; Switzer, C.; Wight, D. *National Action Plan on Demand Response*; Federal Energy Regulatory Commission: Washington, DC, USA, 2010; p. 118.
5. Neukomm, M.; Nubbe, V.; Fares, R. *Grid-Interactive Efficient Buildings: Overview*; U.S. Department of Energy: Washington, DC, USA, 2019; p. 36.
6. U.S. Energy Information Administration Electricity Data. Available online: https://www.eia.gov/electricity/monthly/epm_table_grapher.php?t=epmt_5_01 (accessed on 7 August 2020).
7. Xu, P.; Haves, P. Case Study of Demand Shifting with Thermal Mass in Two Large Commercial Buildings. *ASHRAE Trans.* **2006**, *112*, 572–580.
8. Lee, K.-H.; Braun, J.E. Model-based demand-limiting control of building thermal mass. *Build. Environ.* **2008**, *43*, 1633–1646. [CrossRef]
9. Braun, J. Reducing Energy Costs and Peak Electrical Demand. *ASHRAE Trans.* **1990**, 876–888.
10. Aste, N.; Leonforte, F.; Manfren, M.; Mazzon, M. Thermal inertia and energy efficiency–Parametric simulation assessment on a calibrated case study. *Appl. Energy* **2015**, *145*, 111–123. [CrossRef]
11. Henze, G.P.; Le, T.H.; Florita, A.; Felsmann, C. Sensitivity Analysis of Optimal Building Thermal Mass Control. *J. Sol. Energy Eng.* **2007**, *129*, 473–485. [CrossRef]
12. Turner, W.; Walker, I.; Roux, J. Peak load reductions: Electric load shifting with mechanical pre-cooling of residential buildings with low thermal mass. *Energy* **2015**, *82*, 1057–1067. [CrossRef]
13. Høseggen, R.; Mathisen, H.; Hanssen, S. The effect of suspended ceilings on energy performance and thermal comfort. *Energy Build.* **2009**, *41*, 234–245. [CrossRef]
14. Raftery, P.; Lee, E.; Webster, T.; Hoyt, T.; Bauman, F. Effects of furniture and contents on peak cooling load. *Energy Build.* **2014**, *85*, 445–457. [CrossRef]
15. Wolisz, H.; Kull, T.M.; Streblow, R.; Müller, D. The Effect of Furniture and Floor Covering Upon Dynamic Thermal Building Simulations. *Energy Procedia* **2015**, *78*, 2154–2159. [CrossRef]
16. Gerke, B.; Zhang, C.; Satchwell, A.; Murthy, S.; Piette, M.; Present, E.; Wilson, E.; Speake, A.; Adhikari, R. Modeling the In-teraction Between Energy Efficiency and Demand Response on Regional Grid Scales. In Proceedings of the 2020 ACEEE Summer Study on Energy Efficiency in Buildings, ACEEE, Pacific Grove, CA, USA, 17–21 August 2020.
17. Rabl, A.; Norford, L.K. Peak load reduction by preconditioning buildings at night. *Int. J. Energy Res.* **1991**, *15*, 781–798. [CrossRef]
18. Kintner-Meyer, M.; Emery, A. Optimal control of an HVAC system using cold storage and building thermal capacitance. *Energy Build.* **1995**, *23*, 19–31. [CrossRef]
19. Becker, R.; Paciuk, M. Inter-related effects of cooling strategies and building features on energy performance of office buildings. *Energy Build.* **2002**, *34*, 25–31. [CrossRef]
20. Zhou, G.; Krarti, M.; Henze, G.P. Parametric Analysis of Active and Passive Building Thermal Storage Utilization*. *J. Sol. Energy Eng.* **2005**, *127*, 37–46. [CrossRef]
21. Yang, L.; Li, Y. Cooling load reduction by using thermal mass and night ventilation. *Energy Build.* **2008**, *40*, 2052–2058. [CrossRef]
22. Chen, Y.; Chen, Z.; Xu, P.; Li, W.; Sha, H.; Yang, Z.; Li, G.; Hu, C. Quantification of electricity flexibility in demand response: Office building case study. *Energy* **2019**, *188*, 116054. [CrossRef]
23. Panão, M.J.O.; Mateus, N.M.; Da Graça, G.C. Measured and modeled performance of internal mass as a thermal energy battery for energy flexible residential buildings. *Appl. Energy* **2019**, *239*, 252–267. [CrossRef]
24. Zhang, Y.; Korolija, I. Performing Complex Parametric Simulations with JEPlus. In Proceedings of the SET 2010: 9th Interna-tional Conference on Sustainable Energy Technologies, Shanghai, China, 24–27 August 2010; p. 6.
25. U.S. Department of Energy. EnergyPlus. Available online: https://energyplus.net/ (accessed on 10 August 2020).
26. Chantrasrisalai, C.; Ghatti, V.; Fisher, D.E.; Scheatzle, D.G. Experimental Validation of the EnergyPlus Low-Temperature Radiant Simulation. *ASHRAE Trans.* **2003**, *109*, 614–623.
27. Tabares-Velasco, P.C.; Christensen, C.; Bianchi, M. Verification and validation of EnergyPlus phase change material model for opaque wall assemblies. *Build. Environ.* **2012**, *54*, 186–196. [CrossRef]
28. Mateus, N.M.; Pinto, A.; da Graca, G.C. Validation of EnergyPlus thermal simulation of a double skin naturally and mechanically ventilated test cell. *Energy Build.* **2014**, *75*, 511–522. [CrossRef]

29. Hong, T.; Sun, K.; Zhang, R.; Hinokuma, R.; Kasahara, S.; Yura, Y. Development and validation of a new variable refrigerant flow system model in EnergyPlus. *Energy Build.* **2016**, *117*, 399–411. [CrossRef]
30. U.S. Energy Information Administration, Commercial Buildings Energy Consumption Survey (CBECS). Available online: https://www.eia.gov/consumption/commercial/data/2012/c&e/cfm/c11.php (accessed on 19 February 2019).
31. Deru, M.; Field, K.; Studer, D.; Benne, K.; Griffith, B.; Torcellini, P.; Liu, B.; Halverson, M.; Winiarski, D.; Rosenberg, M.; et al. *US Department of Energy Commercial Reference Building Models of the National Building Stock*; National Renewable Energy Laboratory: Golden, CO, USA, 2011.
32. International Code Council. *2012 International Energy Conservation Code*; International Code Council: Country Club Hills, IL, USA, 2011; ISBN 978-1-60983-058-8.
33. Wilcox, S.; Marion, W. *Users Manual for TMY3 Data Sets*; National Renewable Energy Laboratory: Golden, CO, USA, 2008; p. 58.
34. Integrated Environmental Solutions Ltd, Table 6 Thermal Conductivity, Specific Heat Capacity and Density. Available online: https://help.iesve.com/ve2018/table_6_thermal_conductivity__specific_heat_capacity_and_density.htm (accessed on 6 October 2020).
35. U.S. Department of Energy. Energyplus. *Engineering Reference*; Ernest Orlando Lawrence Berkeley National Laboratory: Berkeley, CA, USA, 2019.
36. Yin, R.; Ghatikar, G.; Piette, M. *Big-Data Analytics for Electric Grid and Demand-Side Management*; Office of Scientific and Technical Information (OSTI): Berkeley, CA, USA, 2019; p. 57.
37. PG&E, Time-of-Use Rate Plans. Available online: https://www.pge.com/en_US/business/rate-plans/rate-plans/time-of-use/time-of-use.page? (accessed on 10 October 2017).
38. Ahn, H.; Freihaut, J.D.; Rim, D. Economic feasibility of combined cooling, heating, and power (CCHP) systems considering electricity standby tariffs. *Energy* **2019**, *169*, 420–432. [CrossRef]
39. Zhu, L.; Hurt, R.; Correia, D.; Boehm, R. Detailed energy saving performance analyses on thermal mass walls demonstrated in a zero energy house. *Energy Build.* **2009**, *41*, 303–310. [CrossRef]
40. Ghoreishi, A.H.; Ali, M.M. Parametric study of thermal mass property of concrete buildings in US climate zones. *Arch. Sci. Rev.* **2013**, *56*, 103–117. [CrossRef]
41. Tsilingiris, P. On the thermal time constant of structural walls. *Appl. Therm. Eng.* **2004**, *24*, 743–757. [CrossRef]
42. Yin, R.; Kara, E.C.; Li, Y.; DeForest, N.; Wang, K.; Yong, T.; Stadler, M. Quantifying flexibility of commercial and residential loads for demand response using setpoint changes. *Appl. Energy* **2016**, *177*, 149–164. [CrossRef]
43. ASHRAE. *2017 ASHRAE Handbook-Fundamentals*; American Society of Heating Refrigerating and Air-Conditioning Engineers, Inc.: Atlanta, GA, USA, 2017; ISBN 978-1-939200-57-0.
44. Kim, D.; Braun, J.; Cliff, E.; Borggaard, J. Development, validation and application of a coupled reduced-order CFD model for building control applications. *Build. Environ.* **2015**, *93*, 97–111. [CrossRef]
45. Ahn, H.; Rim, D.; Lo, L.J. Ventilation and energy performance of partitioned indoor spaces under mixing and displacement ventilation. *Build. Simul.* **2017**, *11*, 561–574. [CrossRef]
46. Korkas, C.D.; Baldi, S.; Michailidis, I.; Kosmatopoulos, E.B. Occupancy-based demand response and thermal comfort optimization in microgrids with renewable energy sources and energy storage. *Appl. Energy* **2016**, *163*, 93–104. [CrossRef]
47. Baldi, S.; Korkas, C.D.; Lv, M.; Kosmatopoulos, E.B. Automating occupant-building interaction via smart zoning of thermostatic loads: A switched self-tuning approach. *Appl. Energy* **2018**, *231*, 1246–1258. [CrossRef]